Prediction of Embankment Failure on Soft Ground

Rupture des Remblais sur Sols Compressibles

T. SHIBATA Professor, Kyoto University, Kyoto, Japan
H. SEKIGUCHI Assoc. Professor, Kanazawa University, Kanazawa, Japan

SYNOPSIS This paper is concerned with the stability control of embankments on soft foundations in conjunction with field measurements of lateral displacements. A method for observationally predicting the impending failure of embankments is proposed and then verified from laboratory loading test results and collected case records. In addition, it is shown that the rate of loading during embanking exerts a profound influence on the ultimate bearing capacity of soft foundations with partial drainage.

INTRODUCTION

Experience with the construction of roads and flood banks on soft foundations has shown that there occurred many embankment failures despite the fact that the factors of safety had been designed to be sufficiently greater than unity (see for example Bjerrum, 1972). One possible approach to avoiding such a failure may be to monitor the field behavior of embankments during construction. In this respect the present study is aimed at proposing a new observational method for predicting the impending failure of embankments on soft ground.

ANALYSES OF SOFT FOUNDATION BEHAVIOR

Lateral deformability factor

Finite element analyses of contained plastic flow of soft foundations with partial drainage under constant rates of embankment loading, have led us to select the lateral deformability factor as an indicator of impending failure of embankments (Sekiguchi and Shibata, 1979 ; Shibata and Sekiguchi, 1980). Here the lateral deformability factor is defined as the ratio of a loading increment (Δq) to the horizontal displacement increment ($\Delta\delta$) at the toe of embankment over a given time period (such as 24 hours) following the commencement of that loading increment (Fig.1).

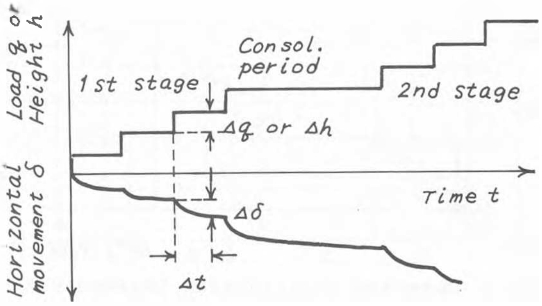

Fig.1 Definitions of symbols used

It may be appropriate here to mention that loading increments during embanking are assumed to be imposed at regular time intervals (the ratio of Δq to Δt is designated hereafter as the loading rate, $\dot{q}$), and that horizontal displacement increments are taken as positive when they are directed away from the embankment. Fig.2 shows calculated relationships between the lateral deformability factor and the intensity of embankment loading (q) at the different values of the coefficient of permeability (k) of the embankment foundation.

Let us first discuss the undrained response represented by the curve with k equal to zero. This curve shows that when the load intensity of 80 KPa is exceeded, the lateral deformability factor tends to decrease linearly with increased load intensity, indicating that the ultimate bearing capacity of the embankment foundation may well be predicted by the point where the linear part of the curve will cross the abscissa. Once an ultimate bearing capacity is thus predicted, it becomes possible to define the degree of impendence of embankment failure in terms of the quantity ($q_f - q$), which is analogous to the remaining life time ($t_f - t$) introduced by Saito (1965) in the case of slope failure.

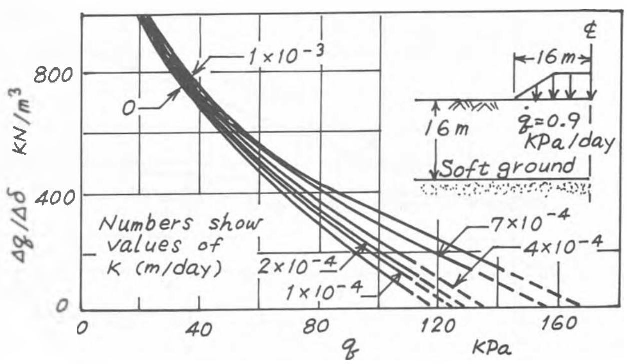

Fig.2 Calculated relationships between lateral deformability factor $\Delta q/\Delta\delta$ and q

From a practical point of view, it should be supplemented that the above mentioned pattern of linearly decreasing $\Delta q/\Delta\delta$ against q holds for partially-drained conditions, as indicated by the curves on Fig.2 with k greater than zero, when the factor of safety (q_f/q) is less than about 1.4.

Influence of loading rate

Fig.3 shows the calculated relationships between the ultimate bearing capacity and the coefficient of permeability at two loading rates. It is evident from the figure that the ultimate bearing capacity tends to increase linearly with increasing coefficient of permeability, when other parameters are held constant. From this finding and related calculations,

$$q_f = q_{fu}\left[1 + C_R \cdot \frac{c_v}{H_d^2} \cdot \frac{q_{fu}}{\dot{q}}\right] \qquad (1)$$

where q_{fu} is the ultimate bearing capacity to be mobilized under undrained conditions, c_v is the coefficient of consolidation, H_d is the maximum drainage distance, $\dot{q}$ is the loading rate and C_R is a proportional constant.

It should be noted that although q_{fu} is also influenced by the loading rate, due to the visco-plasticity of the soil skeleton itself, this influence is found to be opposite in sign and insignificant in magnitude as compared with the partial drainage or consolidation effect (refer again to Fig.3). In the next section the validity of Eq.(1) will be examined based on laboratory loading test results.

LABORATORY LOADING TESTS

Test procedure and equipment

The soil used in the experimental program is fully saturated kaolin having the following index properties: liquid limit=49 %; plastic limit=20 %; and clay fraction=39 %.
The soil was initially prepared in slurry form by adding distilled water to powdered kaolin and by mixing them at a water content of about 80 %.

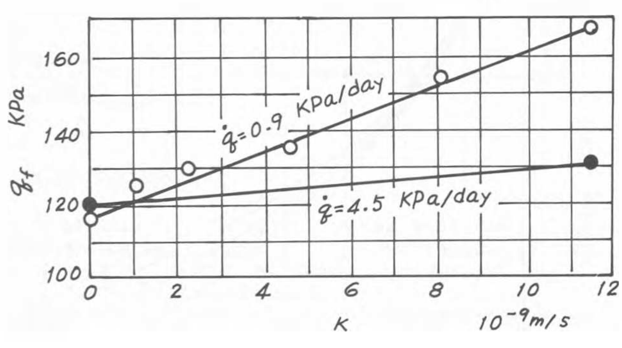

Fig.3 Calculated relationships between ultimate bearing capacity q_f and coefficient of permeability k

The soil slurry was then introduced to the testing vessel (length=200 cm, width=40 cm, height=70 cm) and consolidated one-dimensionally at a vertical pressure of 20 KPa using a water-filled rubber bag. After the completion of consolidation the rubber bag was removed, and immediately following this procedure flexible strip load increments were applied to the surface of the soil layer at regular time intervals, under plane strain conditions. Here the length of the loaded area was 30 cm and the thickness of the soft layer was around 40 cm.

Discussion of test results

Fig.4 summarizes results obtained from four loading tests with different rates of loading. It is seen from Fig.4(b) that each of the four curves exhibits the same pattern as predicted in Fig.2. It is also evident that the ultimate bearing capacities marked by arrows on Fig.4(b) are compatible with the abrupt increase in settlement at the center of loaded area which is observable for each of the four curves on Fig.4 (c).

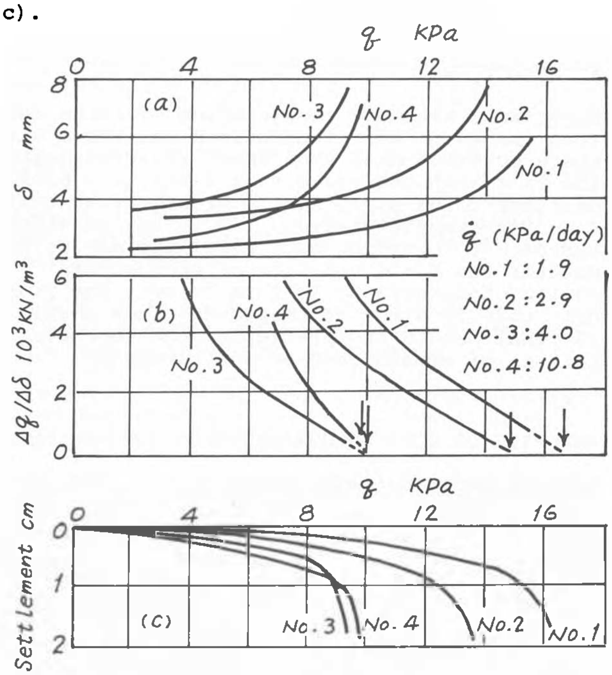

Fig.4 Results of laboratory loading tests

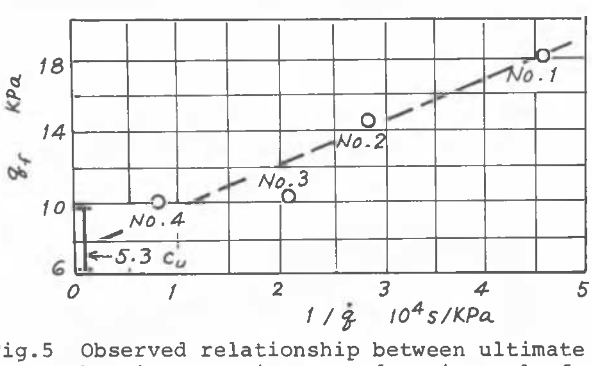

Fig.5 Observed relationship between ultimate bearing capacity q_f and reciprocal of loading rate $1/\dot{q}$

Fig.5 plots the ultimate bearing capacities obtained from Fig.4(b) against the reciprocal of the corresponding rates of loading. It is seen from Fig.5 that there is a linear relationship between q_f and $1/\dot{q}$ which confirms the validity of Eq.(1).

CASE RECORD STUDIES

Shirakawa test embankment

A test embankment was constructed on soft ground at Shirakawa by the Japan Highway Public Corporation (abbreviated as JHPC), for the purpose of assesing the method of stage construction of embankment with no provisions for improving subsoil conditions (the JHPC, 1979).

Principal parameters describing the fill profile and subsoil conditions are listed in Table I, where parameters of other two test embankments explained below are also given.

TABLE I

Parameters of three test embankments

Site	Subsoil conditions				Fill
	soil	depth (m)	w (%)	c_u (KPa)	h (m)
Shirakawa	cohesive	7-11	40-160	5-25	6-8
Kurosaki	cohesive	7	50-400	10-40	6.7
Aiko	organic	3 7	50-250 300-700	5-30	4.5

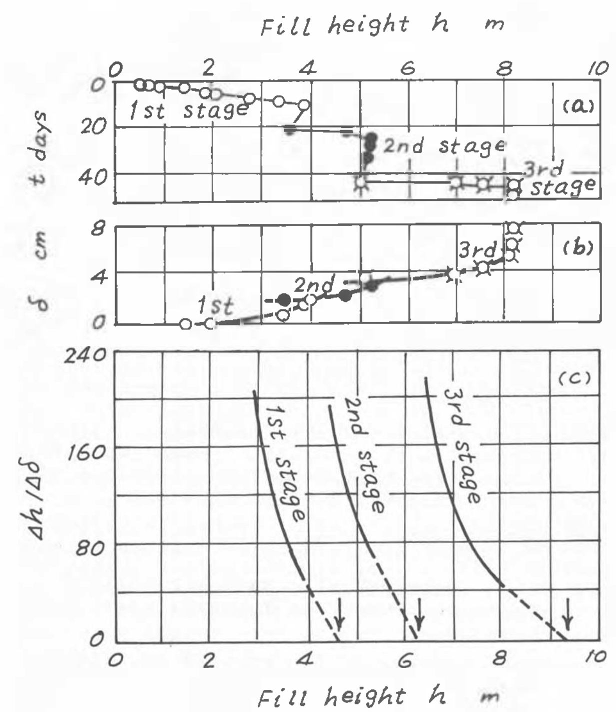

Fig.6 Results from Shirakawa test embankment

Fig.6(a) shows the construction sequence of Shirakawa test embankment. The associated development of horizontal displacement at the toe of the embankment is illustrated in Fig.6(b). The lateral deformability factor is plotted against the fill height in Fig.6(c). Here note that the fill height (h) is used instead of the load intensity, q. It is seen from Fig.6(c) that the same pattern as predicted in Fig.2 holds for each of the three embanking stages. Furthermore, it is noted that such a plot of lateral deformability against fill height is capable of representing the effect of halt time period on the ultimate bearing capacity in a very clear manner.

Kurosaki test embankment

In the case of a test embankment at Kurosaki, sand compaction piles were driven into the foundation soil after the fill height was reduced from 5 m to 2 m, and then embanking was resumed as shown in Fig.7(a) (the JHPC, 1976).

The difference in the horizontal displacement behavior before and after the installation of sand compaction piles can be seen from Fig.7(b). That is, although a considerable amount of lateral soil movement was caused by the driving of the sand compaction piles, the development of horizontal displacement at the second embanking stage was suppressed due to the reinforcement effect of the sand compaction piles. This statement is more clearly seen to be true by plotting the lateral deformability factor against fill height, as indicated in Fig.7(c).

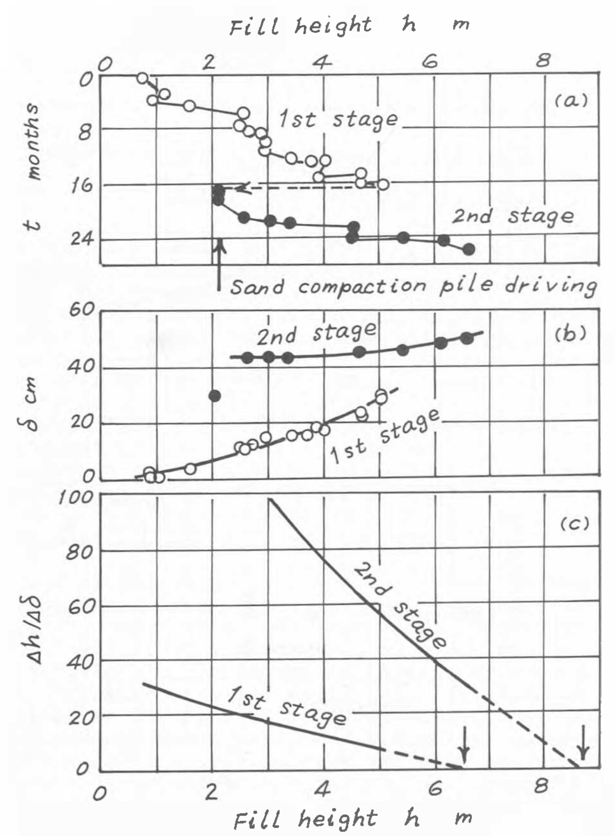

Fig.7 Results from Kurosaki test embankment

Aiko test embankment

This sub-section discusses recorded data of horizontal displacements from two test sections of an embankment constructed at Aiko (the JHPC, 1966). The purpose of the test fill was to evaluate the sand drain performance, and in one section sand drains with a diameter of 40 cm were installed up to 10 m deep at a spacing of 1.2 m in a hexagonal array. In the other section, no provisions for improving subsoil conditions were made for the purpose of comparison.

It is seen from Fig.8(b) that aside from the development of horizontal soil movement due to the installation of the sand drains, δ versus h curves during embanking are similar in shape.

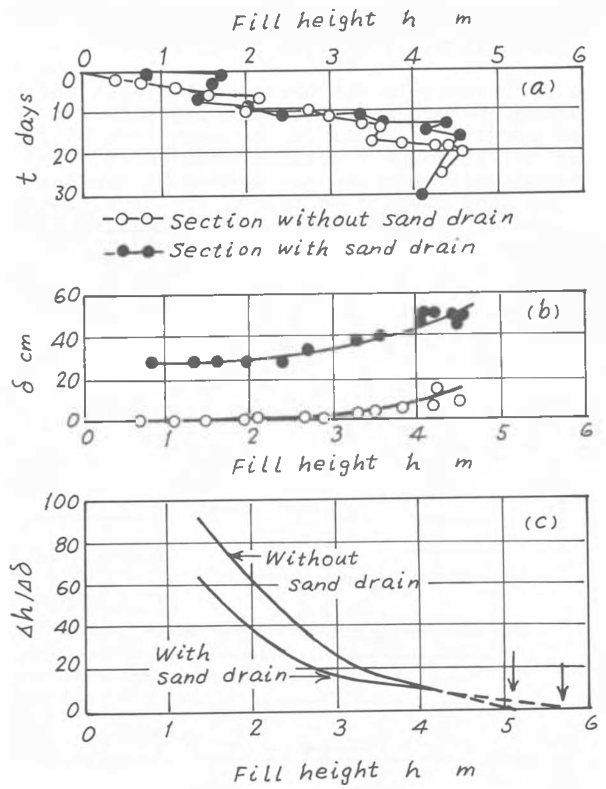

Fig.8 Results from Aiko test embankment

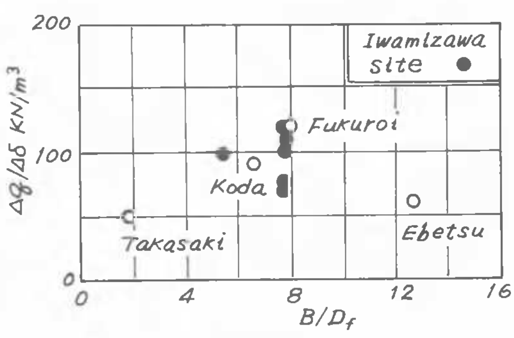

Fig.9 Lateral deformability factors in critical conditions (after Kurihara and Takahashi, 1979)

This implies that in this particular case the sand drain installation did not yield appreciable improvements in the bearing capacity of the soft foundations involved.

A permissible lower limit of $\Delta q/\Delta\delta$

Information on the lateral deformability factor at the onset of crack generation or failure of embankments has recently become available by the work of Kurihara and Takahashi(1979).

Fig.9 shows a plot of lateral deformability factors in such critical conditions against the ratio B/D_f, where B is the base width of embankment and D_f is the maximum depth to a observed sliding surface. From Fig.9, it may tentatively be suggested that further embanking should be halted when the lateral deformability factor ($\Delta q/\Delta\delta$) has reduced to around 200 KN/m^3.

CONCLUSIONS

1. An observational method of predicting the impending failure of embankments, in terms of the lateral deformability factor, has been proposed and verified.
2. The influence of loading rate during embanking on the ultimate bearing capacity of soft foundations with partial drainage has been shown to be expressed as Eq.(1).
3. A permissible lower limit of the lateral deformability factor is tentatively suggested to be equal to 200 KN/m^3, based on the field evidence collected by Kurihara and Takahashi (1979).

REFERENCES

Bjerrum,L.(1972). Embankments on soft ground, Proc. Specialty Cong. Performance of Earth and Earth-Supported Structures, ASCE, (2), 1-54, Lafayette.

Kurihara,N. and Takahashi,T.(1979) Prediction of embankment failures, Proc. 14th Japan National Conf. SMFE, 801-804(in Japanese).

Saito,M.(1965) Forcasting the time of occurrence of a slope failure, Proc. 6th ICSMFE, (2). 537-541, Montreal.

Sekiguchi,H. and Shibata,T.(1979). Undrained behaviour of soft clay under embankment loading, Proc. 3rd Int. Conf. Numerical Methods in Geomechanics, (2), 717-724, Aachen.

Shibata,T. and Sekiguchi,H.(1980). A method of predicting failure of embankment foundation based on elasto-viscoplastic analyses, Proc. of JSCE, 301 (in Japanese).

The Japan Highway Public Corporation (1966). Technical Report on Aiko test embankment.

The Japan Highway Public Corporation(1976). Technical Report on Kurosaki test embankment

The Japan Highway Public Corporation (1979). Technical Report on Shirakawa test embankment.